Finding All Stable Orientations of Assemblies with Friction

Raju Mattikalli, David Baraff, and Pradeep Khosla, *Fellow, IEEE*

Abstract— **Previous work by Mattikalli *et al.* [1] considered the stability of assemblies of frictionless contacting bodies under uniform gravity. A linear programming-based technique was described that would automatically determine a single stable orientation for an assembly (if such an orientation existed). In this paper, we include Coulomb friction at contacts between bodies and give a characterization of the *entire* set of stable orientations of an assembly under uniform gravity. Our characterization is based on the concept of potential stability, which describes a necessary but not sufficient condition for the stability of an assembly. Orientations that are computed as being unstable, however, are guaranteed to fall apart.**

Our characterization reveals that the set of stable orientations maps out a convex region on the unit-sphere of directions and corresponds to a spherical analog of a planar polygon—the region is bounded by a sequence of vertices joined by great arcs. Linear programming techniques are used to automatically find this set of vertices, yielding a description of the range of stable orientations for any assembly. For frictionless assemblies, our characterization of stable orientations is exact. For assemblies with friction, some conservative approximations associated with the use of a linearized Coulomb law are made.

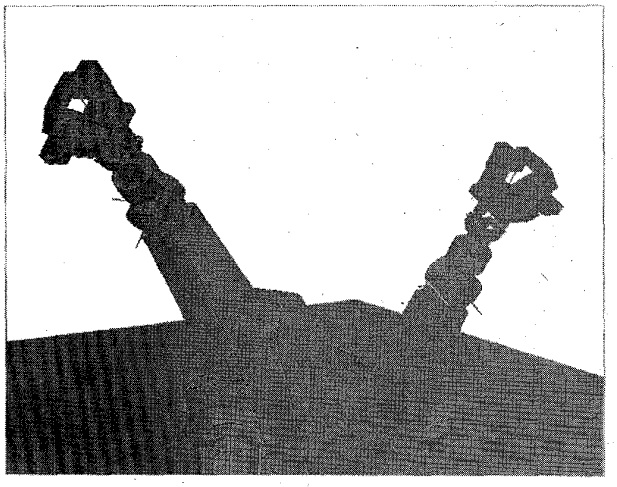

Fig. 1. An assembly held by a gripper on a manipulator. Two poses of the manipulator are shown. The manipulator needs to move the assembly from one pose to the other ensuring that the bodies in the assembly stay in place with respect to each other.

I. Introduction

COMPUTER models of parts and devices are increasingly being used to automate manufacture. In addition, mathematical models of processes are also being used. In situations involving assemblies of objects, models of the mechanics of multiple contacting bodies become important in order to predict the dynamic behavior of the objects during manufacture. For example, during the assembly process, collections of contacting objects are subjected to assembly forces, grasp forces, rapid movements, etc. Fig. 1 shows an assembly held by a robotic manipulator in two different poses. During assembly, the manipulator needs to move the assembly from one position to the other. Note that the gripper on the robotic manipulator is holding only one object in the assembly. In changing the orientation of the assembly, gravitational forces and inertial forces acting on the assembly might upset some of the parts within the assembly, causing them to move relative to other parts. In planning the motion of the manipulator, such movements should be avoided. This requires modeling the dynamics of contacting rigid bodies. There exist systems that automatically generate assembly motion plans using geometric models of parts [2], [3]. However, these systems do not have the capability of modeling the dynamics of the parts during the assembly process.

As a second scenario, consider Fig. 2 which shows a robotic welding setup [4]. A welding torch is mounted at the end of a manipulator and the assembly being welded is mounted on a table top whose orientation can be changed. The planner must find a sequence of table orientations and a trajectory for the robot that ensures collision-free motion for the system during welding. Since the assembly is mounted on the table by clamping one object in the assembly to the table, the planner must also ensure that all the other objects in the assembly remain in place under changing orientations of the table. This paper deals with the stability of objects within an assembly whose orientation is being changed.

In Mattikalli *et al.* [1] the problem of the gravitational stability of an assembly is discussed. The assembly is modeled as a collection of frictionless contacting rigid bodies, one or more of which is assumed to be fixed in place (for example, an object held by a gripper). Such fixed objects are referred to as being *grounded*. Solutions to two problems are presented. The first problem is to determine whether an assembly in a given orientation and subject to a uniform gravity field with direction g is stable. An assembly is defined to be gravitationally stable if all parts of the assembly remain at rest under the influence of the gravity field. The second problem is

Manuscript received June 27, 1994; revised November 2, 1995. This work was supported in part by the Engineering Design Research Center, an NSF Engineering Research Center at Carnegie Mellon University.

The authors are with the Robotics Institute and Engineering Design Research Center, Carnegie Mellon University, Pittsburgh, PA 15213 USA.

Publisher Item Identifier S 1042-296X(96)02577-3.

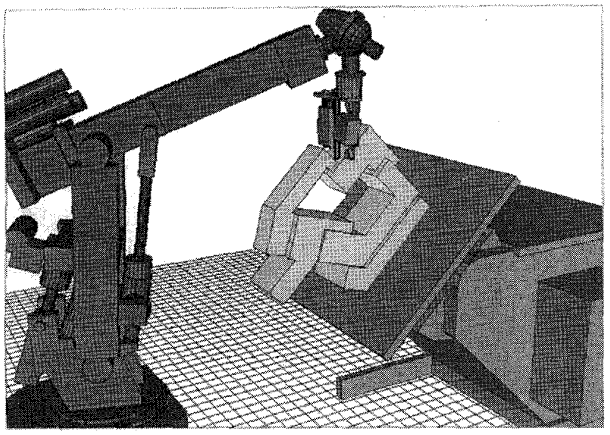

Fig. 2. An assembly mounted on a two-axis welding table. The orientation of the table is changed during welding.

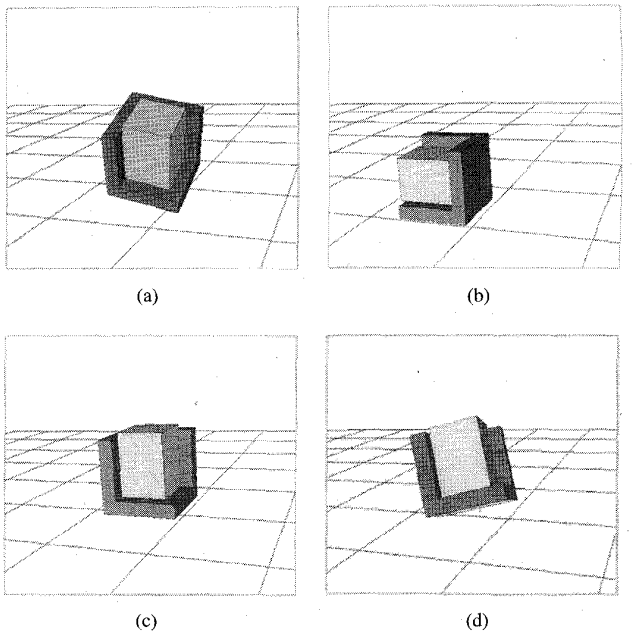

Fig. 3. An assembly in four different orientations with gravity acting downwards perpendicular to the grid. The darker shaded part is grounded. (a) An unstable orientation. (b) and (c) Stable orientations at bounds of stability range. (d) Stable orientation in interior of stability range.

to *find* an orientation of the assembly (if one exists) which is gravitationally stable. A change in orientation of an assembly refers to the rotation of all the parts in the assembly about a fixed axis, keeping g constant. It is simpler, however, to imagine the assembly as existing in some fixed orientation, and considering different gravity directions g which induce gravitational stability. Both problems (determining stability and finding a stable orientation) are shown to be solvable by linear programming. However, the solution method described in this work yields only a single stable orientation, even if many such orientations exist. In this respect, the method fails to provide any characterization or description of the *range* of stable orientations.

This paper presents a method to find the entire range of orientations over which an assembly is gravitationally stable. We begin by first characterizing the shape of the solution space of stable orientations. This characterization shows that the set of unit gravity vectors g which induce stability for an assembly (in a fixed orientation) covers a convex region of the surface of the unit sphere (with the exception of one notable degenerate case). Also, the solution space is contained in a single closed hemisphere, unless it is the entire surface of the sphere itself (the latter implying that the assembly is stable for *any* gravity direction). In addition to being convex, the boundary of the solution region is simply and finitely described. We will show that the shape of the solution region is the spherical analog of a planar polygon; that is, the region's boundary is described as a sequence of vertices, with adjacent vertices connected by great arcs. Our method for describing the range of all stable orientations identifies this set of vertices on the unit sphere, using linear programs similar to those originally described in Mattikalli *et al.* [1].

Having the entire set of stable orientations at hand is clearly more useful than knowing only a single stable orientation. Consider the assembly in Fig. 3(a), where the darker shaded part is fixed in place. This particular orientation is unstable. (For visual simplicity, our illustrations assume a fixed direction of gravity, perpendicular and into the plane of the grid. Different orientations are shown as actual rotations of the assembly itself. As previously stated, however, we view a change of orientation as a variation in the gravity direction, and not the actual parts orientation.) The assembly is, however, stable in a range of orientations, three of which are shown in Fig. 3(b)–(d). The orientation in Fig. 3(b), although stable, is at the boundary of the range of stable orientations, as is the one in Fig. 3(c). A small deviation in the orientation of the assembly away from the stable region will cause the block to move. For this reason, the orientation shown in Fig. 3(d) is superior to those shown in Fig. 3(b) and (c). In selecting a single stable orientation for the assembly, it would be desirable to choose Fig. 3(d). By computing the entire range of orientations over which an assembly is stable, we will be in a position to select the most desirable one—for example one that lies at the "center" of the stable region. If on the other hand, we would like to change the orientation of an assembly during a process, as in the situations of Figs. 1 and 2, then the computed range of orientations can be used to ensure that any change in orientation does not disturb the stability of the assembly.

Unlike the linear programs in Mattikalli *et al.* [1], which were developed for frictionless objects, the linear programs in this paper include friction between parts. However, the inclusion of friction brings with it the problem of *static indeterminacy*; that is, situations in which the stability of an assembly is indeterminate, because the distribution of normal forces is indeterminate. In discussing stability, one can either consider potential stability or guaranteed stability [5]. An assembly is *potentially stable* if contact and friction forces could arise that cause the assembly to remain motionless. On the other hand, an assembly has *guaranteed stability* if *all* contact and friction forces that can arise cause the

assembly to remain motionless.[1] In this paper, we characterize stable orientations of assemblies based on potential stability. Potential stability is discussed in Section II-A. Since potential and guaranteed stability are equivalent for frictionless systems (see Section II-A), our characterization of stable orientations for frictionless assemblies is exact.

The outline of the paper is as follows. In Section II, we describe a linear program that characterizes the set of stable orientations for $\mathbf{g} \in \mathbf{R}^3$. We then show that the restriction of the set to the unit sphere implies the convexity properties described above. In Section III we present a method to compute the boundary of the region of stable orientations. We conclude by showing several examples of assemblies and their computed stable regions.

II. The Set of Stable Orientations

In this section, we show how the set of stable orientations $\mathbf{g}$ for an assembly may be described. At first, we will consider gravity vectors $\mathbf{g}$ of any length in $\mathbf{R}^3$ which cause the assembly to be stable. In general, this large solution set will occupy some volume in $\mathbf{R}^3$. Note that this volume will always include the solution $\mathbf{g} = (0, 0, 0)$; that is, turning gravity to zero makes any assembly stable! To discard this trivial solution, we will then intersect our larger solution volume with the surface of a unit sphere, to discover all unit-length orientation vectors $\mathbf{g}$ which result in stability. In analyzing this intersection, convexity properties of the set of unit-length stable orientations will become apparent.

We begin by finding the set of stable orientations $\mathbf{g}$ of any length in $\mathbf{R}^3$. Fig. 4 shows a set of contacting bodies placed within a gravitational field, with one of the bodies being held fixed. The force of gravity acting on a body with mass M is $M\mathbf{g}$. In addition, contact forces between bodies will also arise. We wish to find gravity vectors $\mathbf{g} \in \mathbf{R}^3$ and resulting contact forces which produce a zero net force on every body in the assembly, meaning that the assembly is in equilibrium.

A. Stability

Determining the stability of contacting frictionless assemblies is relatively straightforward. The acceleration (if any) of a frictionless assembly without contact degeneracies (such as vertex-to-vertex contacts) is unique [8], [6]. In particular, given any external forces acting on the assembly, the stability of the assembly is easily determined. Although the actual contact forces that arise at any given instant may be indeterminate, the overall acceleration of all the bodies is unique. Thus, there is no difference between potential and guaranteed stability, for frictionless systems: If there is any combination of legal contact forces which yields zero acceleration for each body, then *all* legal contact forces will yield zero acceleration for each body. For any assembly, the determination of stability is simply answered by linear programming [9]–[11].

[1] For the special case of frictionless assemblies, the two notions are the same—if a frictionless assembly is potentially stable, it is in fact guaranteed to be stable, assuming well-defined contact normals at contact points [6], [7], [5].

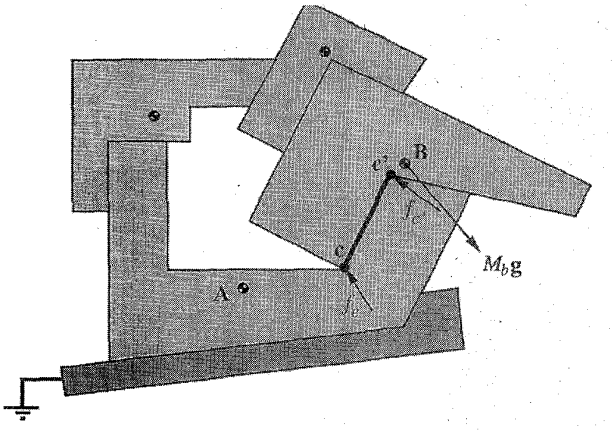

Fig. 4. An assembly in a gravitational field $\mathbf{g}$ of unknown orientation. To find a $\mathbf{g}$ that induces stability in the assembly, equilibrium equations are written for each object.

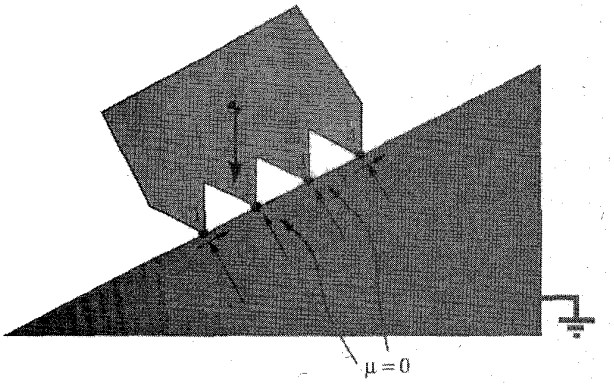

Fig. 5. A block on an incline. Of the four points of contact, the middle two are assumed to have no friction. The forces and accelerations in this situation are indeterminate.

The addition of friction, however, greatly complicates matters. Consider Fig. 5, which shows an object in contact with an inclined plane at a number of points. If the object was frictionless, the distribution of weight among the contact points would be undetermined, but the acceleration would be unique. The object would slide down the plane. Suppose, however, that contact points 1 and 4 have friction, but there is *no* friction at contacts 2 and 3. Now, the behavior is truly indeterminate. If all the weight rests on the interior two contacts, the object will slide down the plane. But if all the weight rests on the exterior two contact points, the object will remain motionless (assuming a large enough coefficient of friction). In fact, there are infinitely many behaviors. If the object's weight is distributed over both the exterior and interior contacts, the acceleration of the object down the plane will be inversely proportional to the weight resting on the exterior contacts.

For friction, there are two approaches we can take to defining stability. We might wish to only consider an assembly stable if it is guaranteed to remain motionless, under any legal distribution of contact forces. In this case, the assembly of Fig. 5 would not be stable. It is not clear how to go about determining if an assembly with friction has guaranteed

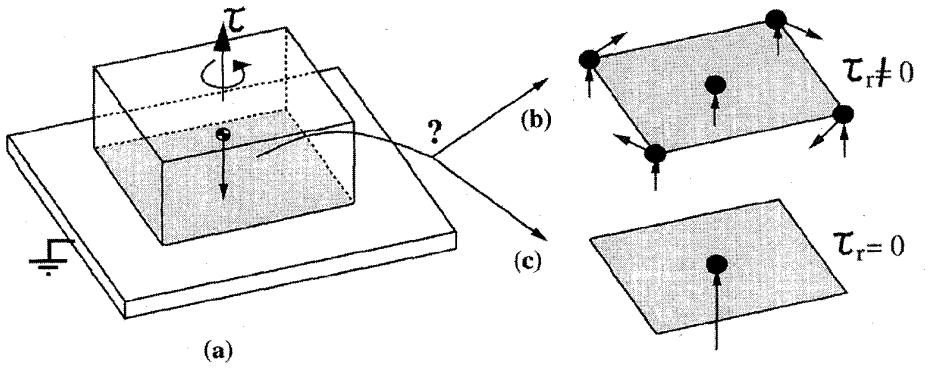

Fig. 6. The problems caused by static indeterminacy in computing stability with friction. (a) A block resting on a grounded table. If the normal forces are distributed at the five contact points, as shown in (b), a frictional torque is generated. However, if the normal force is concentrated at the center, as shown in (c), no torque is generated. The resulting acceleration of the block is hence indeterminate.

stability, without resorting to an exhaustive search method [12], [7].

The second approach, which we will use in this paper, is to declare than an assembly is stable if there exists some legal distribution of contact forces which causes the assembly to remain motionless. This is the concept of potential stability. The assembly in Fig. 5 is potentially stable, since it remains motionless if all the weight rests on the exterior contacts (again, under the assumption that the coefficient of friction is suitably large). Potential stability is easily determined by linear programming [7], [5], [10].

B. The Contact Model

As in Mattikalli *et al.* [1], we model an assembly as a collection of n rigid bodies making polygonal contact (or degenerate polygonal contact) with each other. This allows us to formulate forces at finitely many contact points. A variety of polygonal contact conditions are possible, as shown in Fig. 7(a)–(c) and (e). For frictionless contact, note that in all these situations it is sufficient to model the forces of contact between two bodies as existing at a finite number of points on the boundary of the contact region. For a polygonal contact region as in Fig. 7(a), a linear combination of forces at the five vertices shown are sufficient to produce any contact force that may arise. The same holds true for an edge of contact (Fig. 7(c)) where forces at the two end points of the edge are sufficient.

However, for systems with friction, this leads to some problems because we allow tangential frictional forces to occur only at the finitely many points of contact. To illustrate the problem, consider the example in Fig. 6(a) which shows a block resting on a table with the gravity vector and an external torque τ acting on the block as shown. The contact surface between the block and the table is shown alongside. Let us consider unknown contact forces as occuring at the five points shown in Fig. 6(b). Normal forces arise at the contact points so as to balance the gravitational force. If these forces are distributed over the five contact points, then a nonzero torque can be generated over the surface. However, if the normal forces are such that all the force acts at the center point, as shown in Fig. 6(c), then no torque can be generated. This is the problem of static indeterminacy. In this paper, however, we do not attempt to relax this restriction—we model the contact forces as occuring only at a finite number of contact points on the boundary of contact regions, with tangential forces occuring only at these points. For the following analysis, all the finitely many point contacts over the entire assembly are considered together and indexed from 1 to m.

At each contact point, a surface normal is required. Fig. 7 shows the normal vectors for the different kinds of contact possible. For face-face, face-edge, or face-vertex contact, the normal at any point of contact is well-defined. Fig. 7(b) shows two edges making contact at a point. In this case, the normal vector $\hat{\mathbf{n}}$ is also well-defined and is perpendicular to the two edges as shown. Fig. 7(c) and (e) show degenerate edge-edge and vertex-vertex contacts with ill-defined contact normals. This contact situation makes the problem NP-hard [5]. Being an uncommon situation, we shall assume that a surface of contact with nonvanishing area exists. The orientation of this surface is selected so that the normal direction $\hat{\mathbf{n}}$ lies within the solid, as shown in Fig. 7(d) and (f).

Let $\hat{\mathbf{n}}_i$ denote the unit surface normal at the ith contact point between two bodies A and B, with $\hat{\mathbf{n}}_i$ directed outwards from body B. Let $\hat{\mathbf{u}}_i$ and $\hat{\mathbf{v}}_i$ denote two mutually perpendicular unit vectors in the plane normal to $\hat{\mathbf{n}}_i$; that is, $\hat{\mathbf{u}}_i$ and $\hat{\mathbf{v}}_i$ span the tangent plane at the contact point. The contact force at the ith contact point is decomposed into its components along the three orthogonal directions. Let f_{n_i}, f_{x_i} and f_{y_i} be the signed magnitudes of the force components along $\hat{\mathbf{n}}_i$, $\hat{\mathbf{u}}_i$, and $\hat{\mathbf{v}}_i$, respectively. The net force on body A due to the ith contact is

$$f_{n_i}\hat{\mathbf{n}}_i + f_{x_i}\hat{\mathbf{u}}_i + f_{y_i}\hat{\mathbf{v}}_i \tag{1}$$

while a force of $-f_{n_i}\hat{\mathbf{n}}_i - f_{x_i}\hat{\mathbf{u}}_i - f_{y_i}\hat{\mathbf{v}}_i$ is exerted on body B. Since the normal component of a contact force must be repulsive, and $\hat{\mathbf{n}}_i$ is directed from B toward A, we require that f_{n_i} be nonnegative; that is, $f_{n_i} \geq 0$. There is no sign restriction on f_{x_i} and f_{y_i}; however, Coulomb's law of static friction requires that the magnitude of the tangential force never exceed μf_{n_i}, yielding the restriction

$$f_{x_i}^2 + {f_{y_i}}^2 \leq (\mu f_{n_i})^2 \tag{2}$$

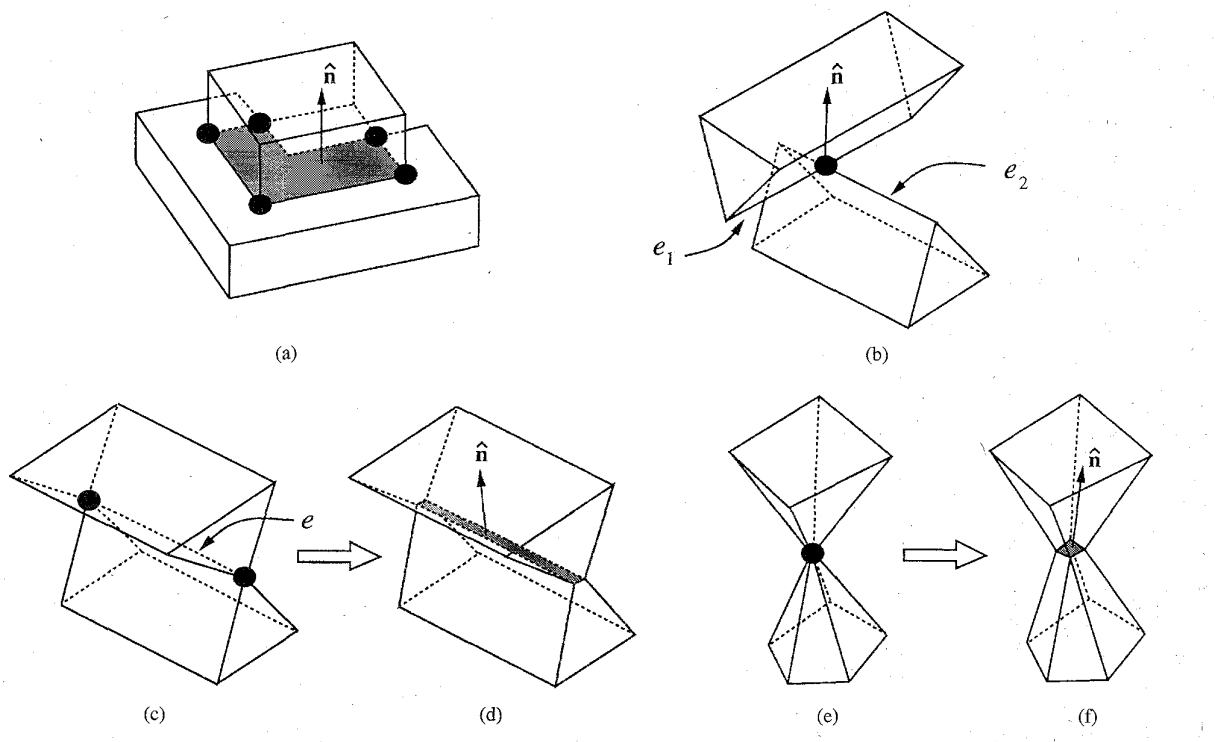

Fig. 7. Different types of contact between bodies. (a) A polygonal surface of contact. (b) Nonparallel edge-edge contact. (c) Degenerate edge-edge contact. (d) Degenerate edge-edge contact resolved by planar approximation. (e) Degenerate vertex-vertex contact. (f) Degenerate contact resolved by planar approximation.

where μ is the coefficient of static friction. (The coefficient of friction may vary at each contact point; however, we will not bother to index μ in this paper, though that is easily done in practice.)

Let us next consider the torques produced by these forces. If the contact occurs at the point $\mathbf{p}_i \in \mathbf{R}^3$, and $\mathbf{c}_a \in \mathbf{R}^3$ denotes the center of mass of body A, then the torque on body A about its center of mass due to the contact force at point i is

$$(\mathbf{p}_i - \mathbf{c}_a) \times (f_{n_i}\hat{\mathbf{n}}_i + f_{x_i}\hat{\mathbf{u}}_i + f_{y_i}\hat{\mathbf{v}}_i). \tag{3}$$

Similarly, the torque acting on body B due to the contact is[2]

$$(\mathbf{p}_i - \mathbf{c}_b) \times (-f_{n_i}\hat{\mathbf{n}}_i - f_{x_i}\hat{\mathbf{u}}_i - f_{y_i}\hat{\mathbf{v}}_i). \tag{4}$$

For an assembly with m contacts, let the vector of normal force magnitudes f_{n_i} be denoted by $\mathbf{f}_n \in \mathbf{R}^m$. Similarly, let $\mathbf{f}_x \in \mathbf{R}^m$ and $\mathbf{f}_y \in \mathbf{R}^m$ denote the vectors of the f_{x_i} and f_{y_i} quantities, respectively. We will denote the generalized force and torque on all n objects of an assembly as a vector $\mathbf{Q} \in \mathbf{R}^{6n}$; the first six components of $\mathbf{Q}$ denote the force and torque acting on body 1, and so on. From (1), (3), and (4), it is obvious that the total force and torque on the n objects depends linearly on $\mathbf{f}_n$, $\mathbf{f}_x$, and $\mathbf{f}_y$. Thus, we can express the generalized contact force $\mathbf{Q}_c \in \mathbf{R}^{6n}$ as the linear expression

$$\mathbf{Q}_c = \mathbf{J}_n^T\mathbf{f}_n + \mathbf{J}_x^T\mathbf{f}_x + \mathbf{J}_y^T\mathbf{f}_y. \tag{5}$$

where $\mathbf{J}_n^T$, $\mathbf{J}_x^T$ and $\mathbf{J}_y^T$ are $6n \times m$ matrices, whose coefficients are determined according to (1), (3), and (4).

[2]For contact between a body A and a grounded object, we can ignore forces acting on the grounded object.

Adding the gravitational force, the net force $\mathbf{Q}$ acting on the assembly is

$$\mathbf{J}_n^T\mathbf{f}_n + \mathbf{J}_x^T\mathbf{f}_x + \mathbf{J}_y^T\mathbf{f}_y + \mathbf{G} \tag{6}$$

where

$$\mathbf{G} = \begin{pmatrix} M_1\mathbf{g} \\ \mathbf{0} \\ \vdots \\ M_n\mathbf{g} \\ \mathbf{0} \end{pmatrix} \tag{7}$$

with M_i being the mass of the ith body in the assembly and $\mathbf{0} \in \mathbf{R}^3$.

C. Conditions for Stability

Given the above notation, we can simply state the necessary conditions for a gravity vector $\mathbf{g}$ to be considered a stable orientation. Since we are considering potential stability, $\mathbf{g}$ is a stable orientation if and only if legal contact forces can arise in response to $\mathbf{g}$ such that the net force and torque on every object is zero. Equivalently, $\mathbf{g}$ is a stable orientation if and only if there exists $\mathbf{f}_n, \mathbf{f}_x$ and $\mathbf{f}_y$ such that

$$\begin{aligned} \mathbf{J}_n^T\mathbf{f}_n + \mathbf{J}_x^T\mathbf{f}_x + \mathbf{J}_y^T\mathbf{f}_y + \mathbf{G} &= \mathbf{0} \\ \mathbf{f}_n &\geq \mathbf{0} \end{aligned} \tag{8}$$

and

$$f_{x_i}^2 + f_{y_i}^2 - (\mu f_{n_i})^2 \leq 0 \quad 1 \leq i \leq m.$$

In (8), all but the set of inequalities corresponding to the Coulomb law of friction are linear. By linearizing these

inequalities, we can make the entire system linear, and hence amenable to solution by linear programming. The geometric interpretation of the inequality

$$f_{x_i}^2 + f_{y_i}^2 - (\mu f_{n_i})^2 \leq 0$$

is that of a right circular cone in the three-space corresponding to f_{x_i}, f_{y_i}, and f_{n_i}, with the axis of the cone along the f_{n_i} axis. A conservative approximation to this cone would be a rectangular pyramid in the interior of the cone as shown in Fig. 8. Since the coefficient of friction μ is rarely known with any great accuracy, we feel that this linearization, which is conservative, is well justified:[3]

$$\begin{aligned} \mathbf{J}_n^T\mathbf{f}_n + \mathbf{J}_x^T\mathbf{f}_x + \mathbf{J}_y^T\mathbf{f}_y + \mathbf{G} &= \mathbf{0} \\ \mathbf{f}_n &\geq \mathbf{0} \\ -\mu f_{n_i}/\sqrt{2} \;\leq\; f_{x_i} &\leq \mu f_{n_i}/\sqrt{2} \quad 1 \leq i \leq m \end{aligned} \tag{9}$$

and

$$-\mu f_{n_i}/\sqrt{2} \;\leq\; f_{y_i} \leq \mu f_{n_i}/\sqrt{2} \quad 1 \leq i \leq m.$$

The set of $\mathbf{g} \in \mathbf{R}^3$ for which there exists $\mathbf{f}_n$, $\mathbf{f}_x$, and $\mathbf{f}_y$ satisfying (9) defines (in general) a volume V. From the definition of $\mathbf{G}$, we have that $(0,0,0) \in V$, because for $\mathbf{g} = \mathbf{0}$, $\mathbf{f}_n = \mathbf{f}_x = \mathbf{f}_y = \mathbf{0}$ clearly satisfies (9). Furthermore, if $\bar{\mathbf{g}} \in V$, so that there exists a solution $\bar{\mathbf{f}_n}$, $\bar{\mathbf{f}_x}$, and $\bar{\mathbf{f}_y}$, then for any scalar $\alpha \geq 0$, we must have $\alpha\bar{\mathbf{g}} \in V$, since $\alpha\bar{\mathbf{f}_n}$, $\alpha\bar{\mathbf{f}_x}$, and $\alpha\bar{\mathbf{f}_y}$ satisfy (9) for $\alpha\bar{\mathbf{g}}$. Because of this, if the solution $\mathbf{g} = (0,0,0)$ is a point in the *interior* of V, then V must be the entire space $\mathbf{R}^3$. Finally, the set V is described in terms of a set of homogeneous linear equalities and inequalities. Therefore V's boundaries (if any) are planes passing through the origin.

D. Characterizing Stable Orientations

Recall, however, that we are really interested in stable orientations (that is, directions). Thus, we would like to consider the intersection of V and the unit sphere; that is, all gravity vectors $\mathbf{g}$ that have unit length and induce stability. We will prove two properties. The first is an interesting property concerning the extent and connectedness of possible stable regions on the unit sphere. It is the following.

Property 1: If the region of stable orientations on the sphere is disconnected, it consists of two antipodal points. Otherwise, the stable region covers the entire sphere, or is contained completely in a closed hemisphere.

We can prove this property by considering the possible forms that the stable volume V might take. There are five possibilities.

1) The set V consists of the origin alone. In this case, the assembly has no stable orientation. This trivially satisfies Property 1.
2) The origin lies in the interior of V. In this case, V is equal to all of $\mathbf{R}^3$, which means that every orientation of the assembly is stable. The stable region covers the entire sphere.

[3]The linearization need not be a rectangular cone; for example, a closer approximation could be obtained by an octahedral cone (at the expense of adding more inequality constraints into (9)). Given the empirical nature of the Coulomb friction model, and the usual uncertainties in the value of μ, a rectangular approximation is likely to be sufficient.

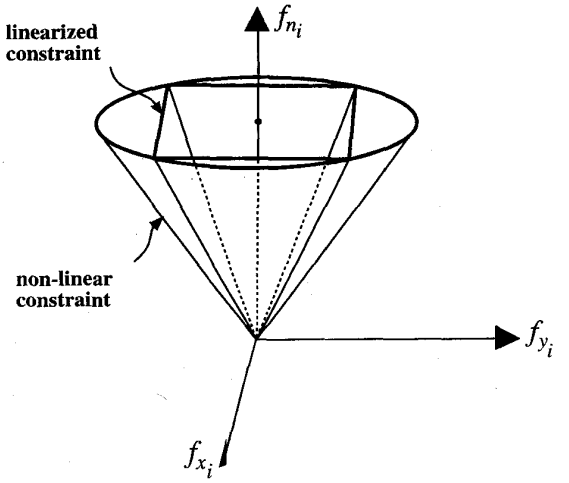

Fig. 8. The nonlinear Coulomb friction constraint is linearized to a square pyramid.

3) The set V corresponds to a line passing through the origin. In this case, there are two stable orientations, represented by a pair of antipodal points on the sphere (Fig. 9(a)).
4) The set V corresponds to an entire plane passing through the origin. The intersection of this plane (since it contains the origin) and the sphere is a single great circle (Fig. 9(b)), which is contained in a closed hemisphere.
5) The set V is a convex cone, possibly planar (Fig. 9(c)).

The first four possibilities for V give rise to a stable region on the sphere that satisfies Property 1. If V is not one of the first four cases, then V is a convex cone emanating from the origin. In this case, the intersection of V with the sphere is contained in a single hemisphere, since the cone is convex.

The second property we wish to show concerns the shape of stable regions and provides the key to planning motions of assemblies as in Fig. 1. It is the following.

Property 2: The region of stable orientations on the sphere is either convex (and therefore connected), or consists of exactly two antipodal points. (We say a region on a sphere is convex if given any two nonantipodal points in the region, the smaller of the two great arcs passing through the two points lies entirely in the region. Under this definition, a single great circle is a convex set on the sphere.)

Property 2 can be proved by contradiction. Let us assume that the stable region on the sphere does not consist of two antipodal points. If the stable region is either empty, the entire sphere, or a great circle, then in each case the region is convex. If the stable region is none of the above, we must show that given any two points in the stable region, there is a great arc that lies between them, every point of which is itself in the stable region. Let $\mathbf{g}_1$ and $\mathbf{g}_2$ be unit vectors denoting two stable points. Since $\mathbf{g}_1$ and $\mathbf{g}_2$ are both stable orientations, they both belong to the larger set V. Since V is convex, consider the line $L \in V$ between them, given in parametric form by

$$L = \mathbf{g}_1 + t(\mathbf{g}_2 - \mathbf{g}_1) \quad 0 \leq t \leq 1. \tag{10}$$

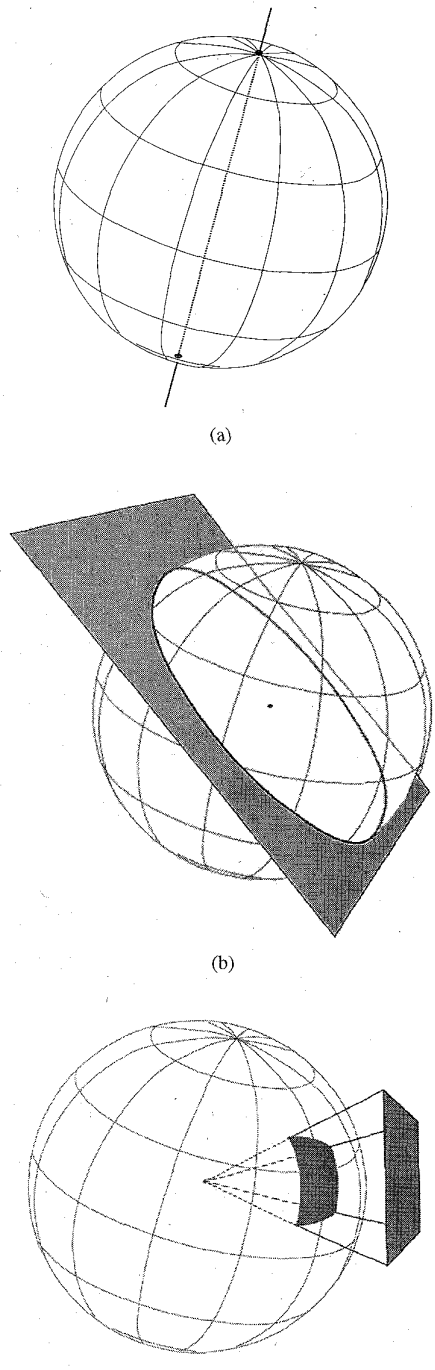

Fig. 9. (a) V is a line, whose intersection with the sphere are a pair of antipodal points. (b) V is a plane, and intersects the sphere over a great circle. (c) V is a convex cone, whose intersection with the sphere is contained in a single hemisphere.

But since for any $\mathbf{g} \in V$ and $\alpha \geq 0$ we have $\alpha \mathbf{g} \in V$, it must be that the great arc A, defined by

$$A = \frac{\mathbf{g}_1 + t(\mathbf{g}_2 - \mathbf{g}_1)}{\|\mathbf{g}_1 + t(\mathbf{g}_2 - \mathbf{g}_1)\|_2} \quad 0 \leq t \leq 1 \tag{11}$$

is also in V, and hence stable. Note that by Property 1, the stable region is contained in a single hemisphere, so $\mathbf{g}_1$ and $\mathbf{g}_2$ cannot be antipodal. This means $\mathbf{g}_1 + t(\mathbf{g}_2 - \mathbf{g}_1)$ is always nonzero, so that A is well-defined. Since A lies on the unit sphere, and also in V, every point in A is by definition in the stable region. This proves Property 2. Property 2 is the most important result of this paper. It shows that if there are two orientations (other than antipodal ones) in which an assembly is known to be stable (for example, two orientations in which an assembly sits on a table), then we are guaranteed to find a series of orientations which will take the assembly from the first orientation to the second ensuring its stability. This result is very useful in assembly planning, as well as a number of other manufacturing tasks.

As a further note, since V's boundaries are planes passing through the origin, the intersection of those planes with the unit sphere are great arcs, and form the boundary of the stable region on the sphere (which we might term a "spherygon.") In the next section, we will show how the vertices of this "spherygon" are found.

III. Finding the Vertices of the Stable Region

We now show how the vertices of the stable region "spherygon" may be found. Essentially, we are looking for the extremal points $\mathbf{g} \in V$, restricted by $\|\mathbf{g}\|_2 = 1$. We can greatly simplify matters if instead of intersecting V with the curved surface of a sphere, we intersect V with the flat surfaces of a unit cube. That is, we consider solutions to (9) with the restriction $\|\mathbf{g}\|_\infty = 1$. (For a vector $\mathbf{v}$, $\|\mathbf{v}\|_\infty = \max_i |v_i|$.) In this case, the intersection of V with any single face of the unit cube is a polygon (or degenerate polygon), rather than a portion of the more complex spherygon. The solutions $\mathbf{g}$ which are the vertices of this polygon, will, when normalized to unit length, be points on the boundary of the spherygon. Each facet of the unit cube produces a polygon which normalizes to a patch on the spherygon. The patches when put together make up the entire spherygon. Vertices of polygons either correspond to a vertex of the spherygon or a boundary of a patch. Note, however, that all vertices of the spherygon will produce a vertex on some polygon. The advantage of this transformation is that it makes the entire problem a problem in linear inequalities, enabling us to use linear programming techniques.

Thus, let us consider instead solutions to (9) such that $\|\mathbf{g}\|_\infty = 1$. Furthermore, in what follows, we will consider only a single face of the unit cube $\|\mathbf{g}\|_\infty = 1$, and without loss of generality, in the remainder of this paper, we will restrict $\mathbf{g}$ by setting $g_x = 1$ and imposing the constraint that $-1 \leq g_y, g_z \leq 1$. Any statements made hereafter about $\mathbf{g}$ assume that they imply in turn to the other five possibilities—$g_x = -1$ and $-1 \leq g_y, g_z \leq 1$, $g_y = 1$ and $-1 \leq g_x, g_z \leq 1$, etc.

Our problem is now to find the vertices of the region on the g_y g_z plane that satisfy

$$\begin{aligned} \mathbf{J}_n^T \mathbf{f}_n + \mathbf{J}_x^T \mathbf{f}_x + \mathbf{J}_y^T \mathbf{f}_y + \mathbf{G} &= \mathbf{0} \\ \mathbf{f}_n &\geq \mathbf{0} \\ -\mu f_{n_i}/\sqrt{2} \leq f_{x_i} &\leq \mu f_{n_i}/\sqrt{2} \quad 1 \leq i \leq m \end{aligned} \tag{12}$$

and

$$-\mu f_{n_i}/\sqrt{2} \leq f_{y_i} \leq \mu f_{n_i}/\sqrt{2} \quad 1 \leq i \leq m$$

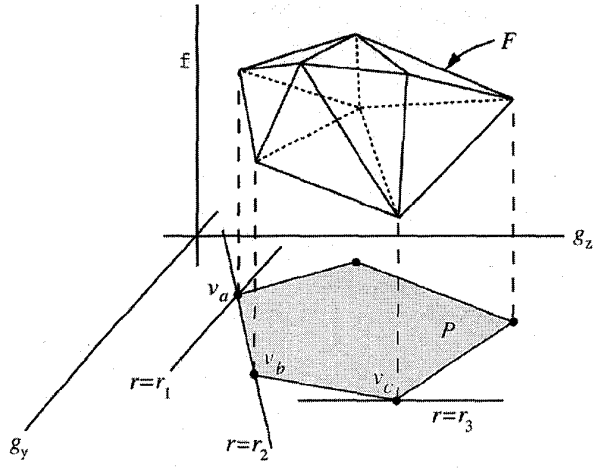

Fig. 10. The projection of the feasible region F onto the $g_y\, g_z$ plane. This projection defines the range of stable orientations.

given the constraints $g_x = 1$ and $-1 \leq g_y, g_z \leq 1$. If we consider the set of feasible solutions $F = (g_y, g_z, \mathbf{f})$ to (12) as the $(3m+2)$-dimensional volume in Fig. 10, we are looking for the vertices of the projection of F onto
This projection is shown as the shaded polygon P in Fig. 10.

Our technique to find the vertices of this projection is as follows. We find an initial vertex of the projection, and then use the technique of *parametric programming* [13] to traverse the perimeter of the projection. Finding an initial vertex of the projection is simple. We first find a solution $(g_y, g_z, \mathbf{f})$ which minimizes g_z (always subject to $-1 \leq g_y, g_z \leq 1$). Note that we are not interested in the value of $\mathbf{f}$ when g_z is minimized; we are only interested in the coordinates (g_y, g_z) at which the minimum occurs. If this first minimization does not uniquely determine both g_y and g_z, we temporarily hold g_z fixed, and find a solution $(g_y, g_z, \mathbf{f})$ which minimizes g_y. In this way, we find some point in F whose projection is a vertex of the polygon P. We will call this initial vertex v_a. (Note that in Fig. 10, the vertex v_a is determined with only a single minimization on g_z.)

Having found an initial vertex of polygon P, we now need to traverse its perimeter. We found our initial vertex (g_y, g_z) of P by minimizing a function of the form

$$C_1 g_y + C_2 g_z \tag{13}$$

shown geometrically in Fig. 10 as the line r. Let us assume that simply minimizing g_z was sufficient to find the initial vertex v_a. In that case, we have performed a minimization with $C_1 = 0$ and $C_2 = 1$ (corresponding to line $r = r_1$) to find v_a. To find the next vertex, suppose that we start increasing C_1. While C_1 is still close to zero, the vertex of P obtained by minimizing (13) will continue to be v_a. However, for some value of C_1, the vertex minimizing (13) will abruptly shift to vertex v_b. Geometrically, as we increase C_1, the line r swings toward the line r_2. At the point that the line r hits r_2, we find another vertex v_b (in addition to v_a) which minimizes (13). We can determine this limit using *sensitivity analysis* [13], a technique of linear programming. This technique finds the range of values that a coefficient of the objective function can

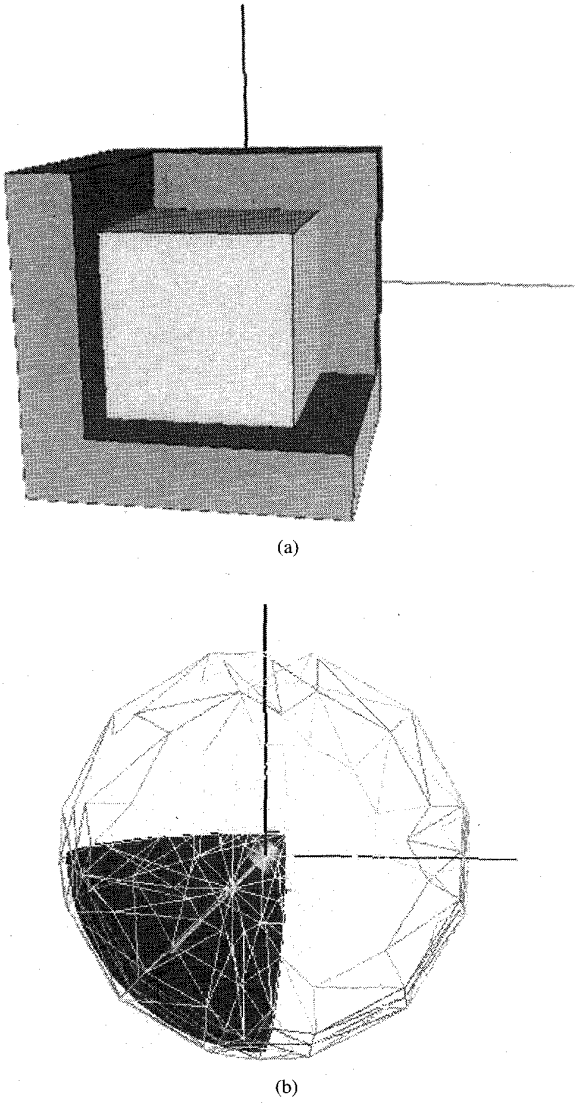

(a)

(b)

Fig. 11. (a) An assembly with the large block grounded. $\mu = 0$. (b) The shaded region on the far side of the sphere (a complete octant of the sphere) indicates all stable orientations.

be varied so as to maintain the same optimal point (the optimal point in this case being v_a). As we continue swinging the line r past r_2, vertex v_a ceases to become a minimizer, and the values of g_y and g_z at v_b are the sole minimizer of (13). By selecting v_b as the new optimal point, further sensitivity analysis can be done to find the next vertex v_c past v_b, and the process can be continued. Notice that after v_c is reached and the value of C_1 is further increased, no new vertices are obtained, inspite of large values of C_1. This corresponds to taking line r close to r_3 which we can see from Fig. 10 will retain the optimal point at point v_c. Now we will have to rotate r past r_3 in order to generate other points on polygon P. To do this, we will need to set $C_1 = 1$ and change values of C_2. This process is continued to obtain the rest of the vertices of P. Eventually, we will find ourselves back at the original vertex v_a, and the traversal is stopped. Note that this procedure is quite similar to the steps of the simplex algorithm for linear programming.

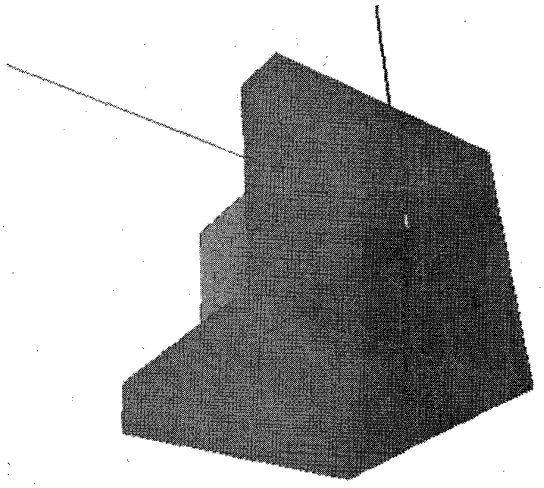

(a)

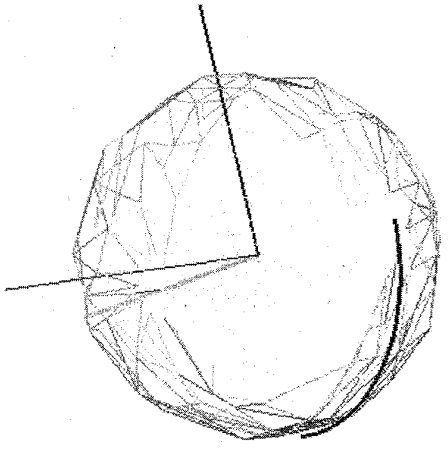

(b)

Fig. 12. (a) An assembly with the L-shaped bracket grounded. $\mu = 0$. (b) The dark line on the sphere shows all stable values for $\mathbf{g}$.

Having found the vertices of the stable region on all faces of the unit cube, it is trivial to transform those vertices to the unit sphere and map out the stable region on the sphere. In Figs. 11 through 16, we present some sample assemblies and their stable regions shown shaded on the surface of a sphere. In each figure, on the left is shown an assembly with its grounded object shaded darker. On the right, a wireframe of a sphere is shown, with dark patches corresponding to the stable orientations of the assembly. To locate the stable region with respect to the assembly, the same coordinate frame is used on the assembly and on the sphere.

In the examples presented in Figs. 11 and 12, the coefficient of static friction has been selected to be zero. Fig. 11 consists of a cube sitting within a concavity in a grounded block. The stable region is defined by the patch shown on the far side of the sphere. Note that this patch covers an octant defined by the 3 negative coordinate directions (the positive coordinate directions are shown in the figure). Fig. 12(a) shows a block that is placed within a grounded L-shaped bracket. The stable region corresponds to a line as shown on the sphere in Fig. 12(b).

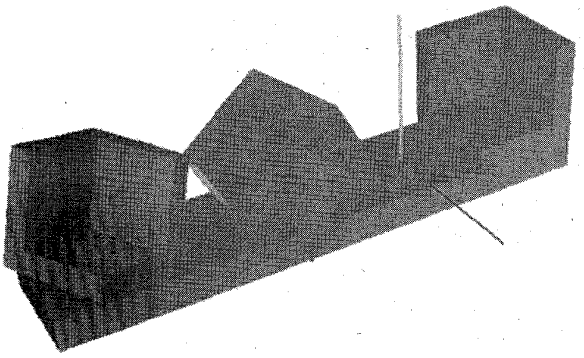

(a)

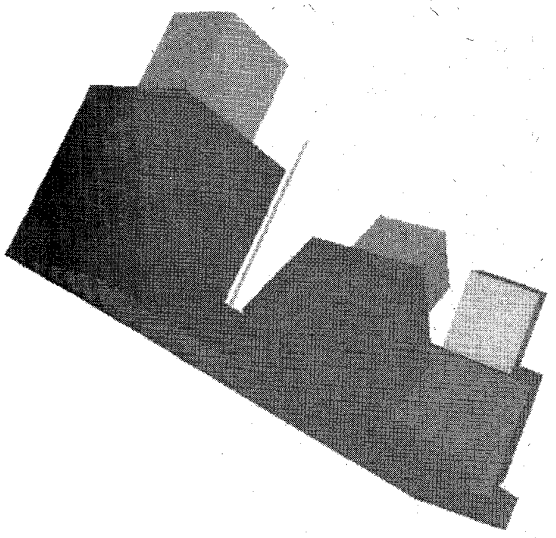

(b)

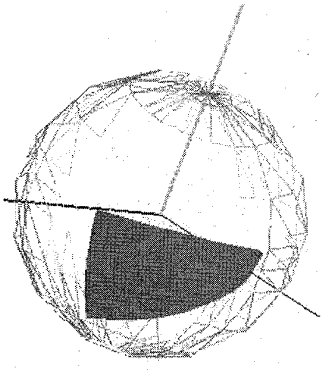

(c)

Fig. 13. (a) The grounded part of an assembly. A cube is placed in each of the cubicals. (b) The assembly consisting of a total of four parts. (c) The shaded region on the sphere shows stable $\mathbf{g}$'s for $\mu = 0$.

Fig. 13 shows an example where the stable region is less than an entire facet. The large parts with 3 hollows is the grounded part. Here again the coefficient of friction is selected

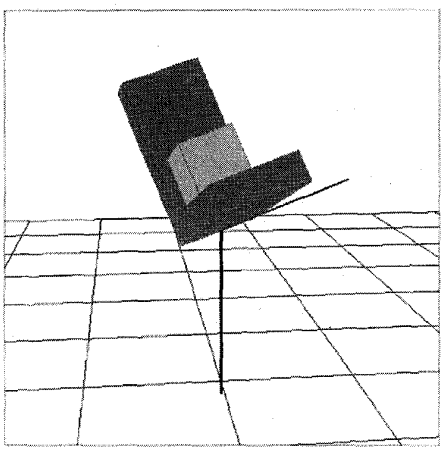

(a)

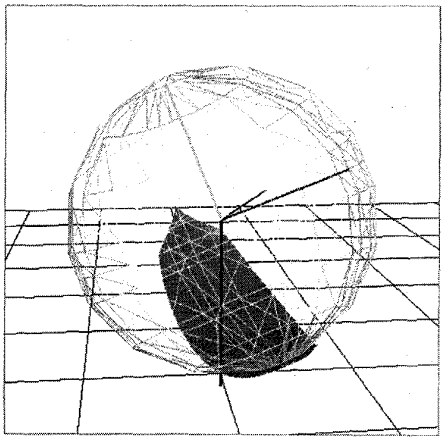

(b)

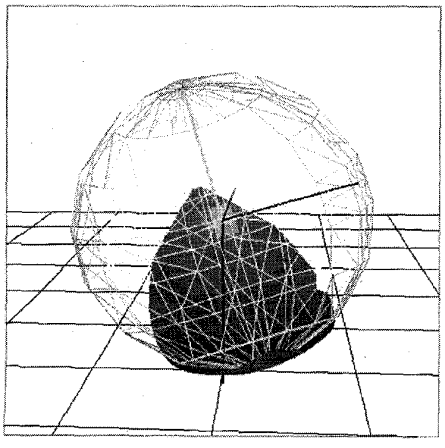

(c)

Fig. 14. (a) An assembly with the L-shaped part grounded. (b) The shaded areas show stable $\mathbf{g}$'s with $\mu = 0.2$. (c) Stable region with $\mu = 0.4$.

to be zero. It is shown separately for clarity in Fig. 13(a). Fig. 13(b) shows the assembly wherein 3 cubes are placed within the 3 hollow cubical spaces. The stable region is shown in Fig. 13(c).

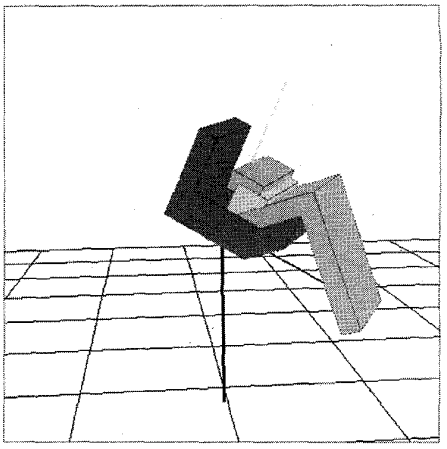

(a)

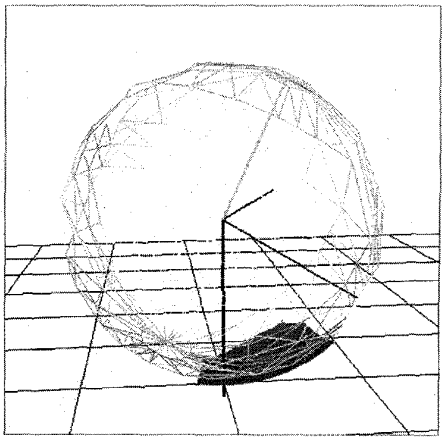

(b)

Fig. 15. (a) An assembly with the dark U-shaped part grounded. $\mu = 0.2$. (b) The shaded area shows stable $\mathbf{g}$'s.

Fig. 14 considers the assembly of Fig. 12, this time with a nonzero coefficient of static friction μ. Fig. 14(b) shows the stable region when $\mu = 0.2$, while (c) shows the region for $\mu = 0.4$. The stable region has grown from a line in Fig. 12(b) to a patch in Fig. 14(b). As expected, in the presence of friction, the assembly can be tilted by a small amount in the direction perpendicular to the plane of the L-shape.

Fig. 15 shows a multipart assembly and its stable region for $\mu = 0.2$.

As a final example, consider the assembly in Fig. 16(a). The stable region shown in Fig. 16(b) corresponds to a zero coefficient of friction. This is an obvious result. What is not so obvious is the stable region obtained for a coefficient of friction of $\mu = 0.3$ as shown in Fig. 16(c). One expects to see a nonconvex region on the sphere covering more than a hemisphere, but not the entire sphere. Instead what we obtain is a solution corresponding to the entire sphere. To explain this apparent incorrect solution, we must reexamine our choice of potential stability concepts in computing these stable regions. As stated earlier, we declare any orientation of an assembly as being stable if we can find a set of contact

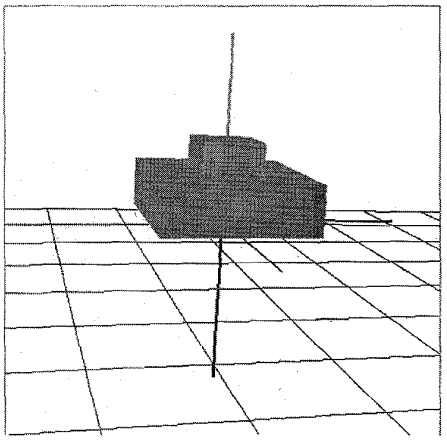

(a)

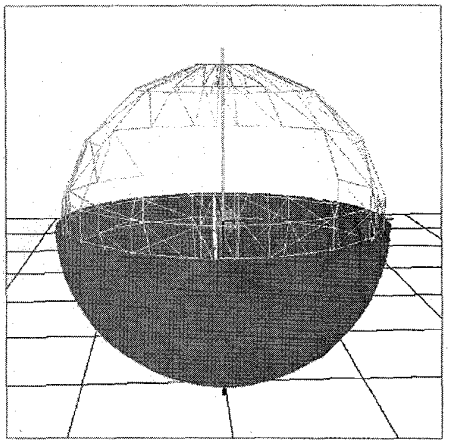

(b)

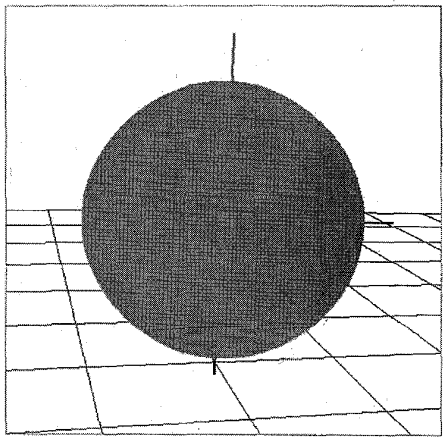

(c)

Fig. 16. (a) An assembly with the shaded part grounded. (b) The shaded area shows stable $\mathbf{g}$'s with $\mu = 0.0$. (c) Stable region with $\mu = 0.3$.

forces that satisfy the equilibrium equations in (12). Consider the nongrounded block in Fig. 16(a). It can be seen that an arbitrary contact force can be assumed to be acting over one of the side contact faces of the block since the force can be balanced by an equal and opposite force on a parallel contact face. As a result, sufficient frictional forces can be generated on the two parallel faces (in keeping with the constraints in (12)) to oppose an upward gravitational force on the block. This makes the upward gravitational direction a stable one, resulting in the closed sphere of Fig. 16(c). This result is a consequence of choosing potential stability as the criterion for finding stability. As indicated earlier, the alternative guaranteed stability criterion is very hard to employ, since it requires complete enumeration of all possible force distributions. As future work, it would be interesting to explore the possibility of a more precise criterion for stability.

IV. Conclusion

In modeling assemblies to plan for product manufacture, it becomes necessary to be able to predict their mechanics under external forces such as gravitational forces, fixturing forces and machining forces. Typically, it is desired that the parts remain motionless. In this paper we present a method of finding *all* the potentially stable orientations in which an assembly can be placed within a uniform gravity field. The method extends earlier work which found a single stable orientation. To find all stable orientations, the proposed method solves for the projection of the entire set of feasible solutions of a high-dimensional linear program onto a two-dimensional plane. Stable orientations are mapped onto regions on the surface of a sphere. For a given assembly, the mapping of stable regions onto the surface of a sphere can be graphically displayed. This mapping can be used during assembly process planning. Any subassembly that is being manipulated, or placed on a table, or within a fixture, can now be placed in an orientation that keeps the subassembly stable. The dimension of the linear program is given by the number of contact points. The stable orientations of an assembly with 100 contact points is solvable in well under a second of CPU time on a DEC 5000.

As future work, we plan to explore stability criteria other than the potential stability criterion that we have used in this paper. Also we are investigating more closely the interrelation between the stable regions and grasp/fixture planning. This would allow us to generate fixture plans that produce desired stability regions.

Acknowledgment

The authors would like to thank H. Sutioso who developed the code for rendering patches on the surface of a sphere. They would also like to thank the reviewers of this paper, whose comments and suggestions have contributed significantly to the paper.

References

[1] R. Mattikalli, D. Baraff, B. Repetto, and P. Khosla, "Gravitational stability of frictionless assemblies," *IEEE Trans. Robot. Automat.* vol. 11, no. 3, pp. 374–388, 1995. Also available as CMU Rep. CMU-RI-93-13, Carnegie Mellon Univ., Pittsburgh, PA, 1993.

[2] R. Mattikalli, P. Khosla, and Y. Xu, "Subassembly identification and motion generation for assembly: A geometrical approach," in *Proc. IEEE Conf. System Engineering*, 1990, pp. 399–403.

[3] R. Wilson, "On geometric assembly planning," Ph.D. dissertation, Stanford Univ., Stanford, CA, Mar. 1992.
[4] J. S. Hemmerle, M. Terk, E. L. Gursoz, F. B. Prinz, and T. E. Doyle, "Next generation manufacturing task planner for robotic arc welding," *ISA Trans. AI Eng. Design Manufact.*, vol. 31, no. 2, pp. 97–114, Apr. 1992.
[5] R. S. Palmer, "Computational complexity of motion and stability of polygons," Ph.D. dissertation, Dep. Comput. Sci., Cornell Univ., Ithaca, NY, May 1989.
[6] R. Cottle, "On a problem in linear inequalities," *J. London Math. Soc.*, vol. 43, pp. 378–384, 1968.
[7] D. Baraff, "Issues in computing contact forces for nonpenetrating rigid bodies," *Algorithmica*, vol. 10, pp. 292–352, 1993.
[8] W. Ingleton, "A problem in linear inequalities," in *Proc. London Mathematical Society*, 1966, vol. 16, no. 3, pp. 519–536.
[9] J. C. Trinkle, "On the stability and instantaneous velocity of grasped frictionless objects," *IEEE Trans. Robot. Automat.*, vol. 8, no. 5, pp. 560–572, Oct. 1992.
[10] M. Blum, A. Griffith, and B. Neumann, "A stability test for configurations of blocks," Mass. Inst. Technol., Cambridge, Tech. Rep. AI Memo. 188, Feb. 1970.
[11] R. Mattikalli, P. Khosla, B. Repetto, and D. Baraff, "Stability of assemblies," in *Proc. IEEE/RSJ Int. Conf. Intelligent Robots and Systems*, Yokohama, Japan, July 1993, pp. 652–661.
[12] M. Erdmann, "On motion planning with uncertainty," Master's thesis, Mass. Inst. Technol., Cambridge, 1984.
[13] V. Chvatal, *Linear Programming*. New York: Freeman, 1983.

Raju Mattikalli received the B.Tech. degree in mechanical engineering from the Indian Institute of Technology, Bombay, India, in 1987 and the M.Eng. and Ph.D. degree in mechanical engineering from Carnegie Mellon University, Pittsburgh, PA, in 1989 and 1994, respectively. His research interests lie in the areas of computer-aided design and manufacture, which include topics in design for manufacture, geometry based planning, mathematical simulation of manufacturing processes, and geometric modeling. His dissertation work was on mechanics-based assembly planning using geometric models of parts. Currently, he is a Postdoctoral Research Associate at the Engineering Design Research Center at Carnegie Mellon.

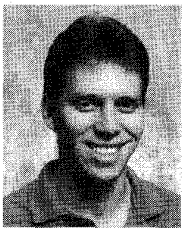

David Baraff received the Bs.E. degree in computer science from the University of Pennsylvania, Philadelphia, in 1987. He received the Ph.D. degree from Cornell University, Ithaca, NY, in 1992, where he was a graduate student in Cornell's Department of Computer Science and Program of Computer Graphics.

Before and during his undergraduate studies, he was with AT&T Bell Laboratories' Computer Technology Research Laboratory doing computer graphics research, including real-time 3-D interactive animation and games. After receiving the Ph.D. degree, he joined the faculty of Carnegie Mellon University, Pittsburgh, PA, in 1992 as an Assistant Professor in CMU's Robotics Institute and also the School of Computer Science. In 1995, he was named an ONR Young Investigator. His research interests include physical simulation and modeling for computer graphics, robotics, and animation.

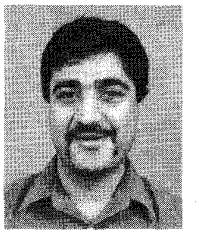

Pradeep Khosla (S'83–M'83–SM'91–F'95) received both the M.S. and Ph.D. degrees from Carnegie Mellon University, Pittsburgh, PA.

He is Professor of Electrical and Computer Engineering at Carnegie Mellon. He is also a member of the the Robotics Institute and Director of Advanced Manipulators Laboratory. Currently, he is on leave from Carnegie Mellon and is serving as a Program Manager in the Software and Intelligent Systems Technology office at ARPA, where he is responsible for programs in manufacturing and real-time software and planning. Prior to joining Carnegie Mellon, he was with Tata Consulting Engineers and Siemens in the area of real-time control.

Dr. Khosla's research interests are in the area of real-time sensor-based manipulation, reusable software for real-time control and real-time operating systems, modular manipulators, integrated design-assembly systems, and robotic applications in space, field, and manufacturing environments. He is involved in electrical and computer engineering and robotics education both at the graduate and the undergraduate level.

Dr. Khosla was a member of the committee that formulated a curriculum for the Ph.D. program in robotics at Carnegie Mellon. He was also a member of the Wipe the Slate Clean Committee that created a new four-year undergraduate ECE degree curriculum at Carnegie Mellon. He is the chairman of the Education Committee of the IEEE Robotics and Automation Society. He was elected Fellow of the IEEE in 1995 for contributions in reconfigurable manipulators and reconfigurable software for sensor-based control and for leadership in curriculum development.